JETIR.ORG ISSN: 2349-5162 | ESTD Year : 2014 | Monthly Issue
JOURNAL OF EMERGING TECHNOLOGIES AND INNOVATIVE RESEARCH (JETIR)
An International Scholarly Open Access, Peer-reviewed, Refereed Journal

Synthesis and Characterization of Conducting Polypyrrole Based Composites with SnO_2 to Sense NH_3 Gas at room temperature

R.P. Ikhar[1], G. T. Lamdhade[2], K. B. Raulkar[2]
[1]Vidya Bharati Madhyamik Vidyalaya, Patrakar Colony, Amravati
[2]Department of Physics, Vidya Bharati Mahavidyalaya, Camp, Amravati
Corresponding Author email: kbraulkar2016@gmail.com

Abstract:
PPy-SnO_2 ammonia gas sensor was fabricated using Al_2O_3 base on clean glass plate. The prepared material was characterized using X-ray diffraction and Scanning electron Microscopy. From XRD, it was found that composition $40SnO_2$:60PPy (sensor N4) exhibits a smaller crystallite size (38.2 nm) due to the significant influence of the higher concentration of polypyrrole (PPy) in the composite. SEM picture exhibited the particle size of N4 sensor is in the range of 20 - 40 nm with very high porosity due to open, sponge-like porous network morphology. Due to high porosity and enhanced surface reactivity, N4 sensor exhibited the highest sensitivity, reaching approximately 1.45 at 70 ppm.

Keywords: SnO_2-PPy composites thick layer, Al_2O_3, Screen Printing Technique, sensitivity.

I. Introduction:

Because of their exceptional qualities and technological uses, nanostructure metal oxides have garnered a lot of interest. The size, shape, and structure of nanoparticles have a significant impact on the electrical, magnetic, optical, and catalytic capabilities of nanomaterials. The fact that nanoparticles react differently from bulk materials is another factor drawing scientists' attention to them. The semiconductors' band structure varies as the particle size decreases. Band edges break into lower energy levels when the band gap widens [1-2].

Due to its exceptional electrical conductivity, chemical stability, and capacity for reversible doping, polypyrrole (PPy) is essential for ammonia (NH_3) gas detection. The movement of positive charge carriers (holes) produced during oxidative doping is the source of electrical conduction in PPy, a p-type conducting polymer. Since NH_3 contributes electrons to the polymer backbone, PPy experiences a dedoping reaction when exposed to ammonia, a basic gas. Electrical resistance decreases as a result of this electron donation's reduction of the hole concentration. Quantitative detection is made possible by the correlation between the resistance change's magnitude and the NH_3 concentration. Faster response and recovery times are the consequence of PPy's high surface area and porous structure, which improves gas adsorption and speeds up the interaction between NH_3 molecules and the polymer. Additionally, its flexibility and processability allow PPy to be used alone or as a

composite with metal oxides (e.g., SnO_2, ZnO) to improve sensitivity, selectivity, and stability for industrial and environmental ammonia monitoring [3-5].

II. Experimental

A. Synthesis of SnO_2 Nanoparticles:

The GR grade chemicals utilized in the aforementioned study were acquired from Sd-fine, India (purity 99.99%). SnO_2 was prepared by dissolving 2g (0.1 M) of stannous chloride dehydrate ($SnCl_2.2H_2O$) in 100 ml of water. Approximately 4 ml of ammonia solution was added to the foregoing aqueous solution with magnetic stirring once it had completely dissolved. For twenty-five minutes, stirring was maintained until a white gel precipitate developed [6-7].

After that, it was left to settle for ten to fourteen hours. Following that, it was filtered and given four to five water washes using de-ionized water. The resulting precipitate was combined with 0.27g of charcoal-activated carbon black powder. To turn the mixer into a powder, it was placed in a vacuum oven set at 80 degrees Celsius for approximately one day. A grinder was then used to grind this dry substance into a fine powder. To fully remove the impurities from the product, this fine product of SnO_2 nanopowder was calcined at 700^oC for seven hours in an auto-controlled muffle furnace (Gayatri Scientific, Mumbai, India).

B. Synthesis of Polypyrole (PPy):

PPy was synthesized using methanol, anhydrous iron (III) chloride ($FeCl_3$), and the Py monomer [10]. First, a round-bottom flask containing 7 ml of methanol and 1.892 g of $FeCl_3$ was made. The ($FeCl_3$+methanol) solution was then continuously stirred in the dark while 8.4 ml of Py monomer was added. Py monomer was added to the solution in a ratio of 1/2.33 times that of $FeCl_3$ in order to maximize yield. The black precipitates that resulted were filtered and thoroughly cleaned with distilled water until they were clear. The resulting PPy was dried for three hours at 600 degrees Celsius in an oven [8-9].

C. Fabrication of thick films:

The screen printing method was used to create thick films of the produced samples. First, a solution of ethyl cellulose (as a 10% temporary binder) in a mixture of organic solvents like butyl cellulose, butyl carbitol acetate, and turpineol was mixed with the sintered fine powder of pure and composite nano-powder of SnO_2 and PPy in varying weight percentages to create the thixotropic paste for screen printing. When creating the paste, the proportion of inorganic to organic ingredients was maintained at 75:25. After that, the paste was utilized to create thick layers of SnO_2 and PPy pure and composite materials, which were then screen printed onto a glass substrate that had been cleaned and had Al_2O_3 as the basis.

In order to evaporate all organic ingredients (in the form of binders) and organic contaminants, the produced films were dried in an oven set to 90 to 100 degrees Celsius for one hour. Silver paint electrodes were created on the films' adjacent surfaces for the surface conductance measurement, and the films were once more heated to 70 degrees Celsius for 30 minutes to dry the silver paint [10]. The series of samples are as shown in the table 1.

Table 1: Series Label

Sr. No.	Sensor codes	Layers
1.	N1	100SnO_2/ Al_2O_3/GP
2.	N2	80SnO_2: 20PPy / Al_2O_3/GP
3.	N3	60SnO_2: 40PPy / Al_2O_3/GP
4.	N4	40SnO_2: 60PPy / Al_2O_3/GP
5.	N5	20SnO_2: 80PPy / Al_2O_3/GP
6.	N6	100PPy / Al_2O_3/GP

III. Results and Discussions:

A. XRD (X-ray Diffraction) Study:

The XRD pattern of pure polypyrrole (PPy) typically exhibits a broad, diffuse peak rather than sharp, well-defined diffraction peaks, indicating its amorphous nature. Graph showed a broad hump centered around 20°–30° (2θ) is characteristic of the disordered arrangement of PPy chains. This diffuse scattering arises from the short-range ordering between polymer chains and the absence of long-range periodicity, which is a defining trait of amorphous materials. The lack of sharp peaks confirms that polypyrrole does not form a well-ordered crystalline lattice but instead exists in a structurally irregular, amorphous state. This disordered structure is typical for conducting polymers and plays a crucial role in their electrical, electrochemical and gas sensing behavior [11-12].

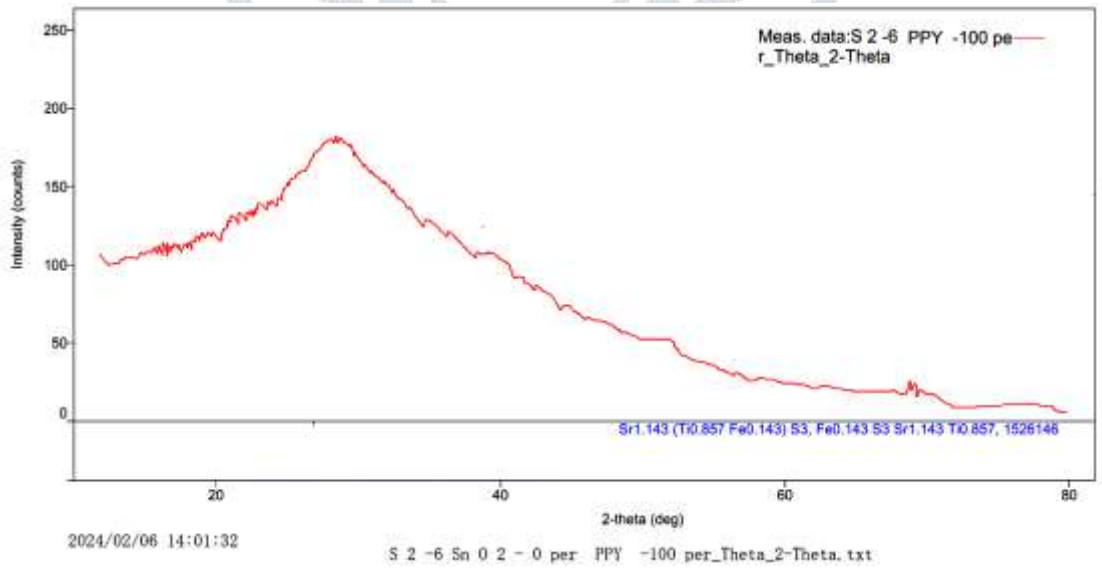

Fig. 1 : XRD pattern of PPy

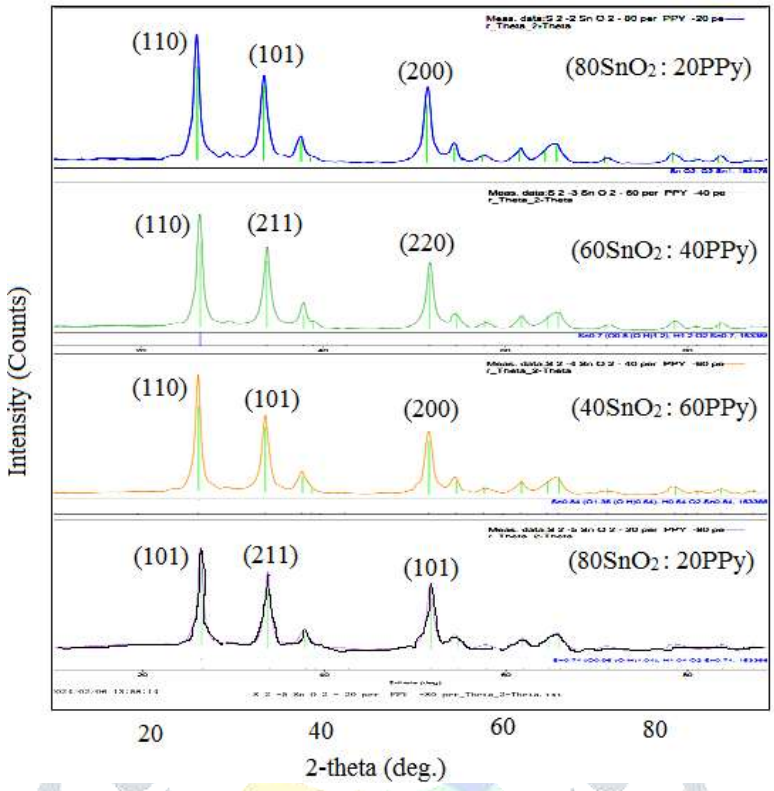

Fig. 2 : XRD pattern of SnO_2+ PPy composites

Table 2: Average crystallite size of SnO_2, PPy and their compositions

Sensor Codes	Chemical Composition of SnO_2: PPy (mole %)	Maximum Intensity Peak Position (2θ) degree	FWHM (2θ) degree	Average Crystallite Size (D) in nm
N1	100SnO_2:00 PPy	26.54	0.103	77.4
N2	80SnO_2:20 PPy	26.46	0.129	61.8
N3	60SnO_2:40 PPy	26.499	0.142	56.2
N4	40SnO_2:60 PPy	26.52	0.209	38.2
N5	20SnO_2:80 PPy	26.45	0.184	43.4
N6	00SnO_2:100 PPy	26.63	0.127	64.26

The composition 40SnO_2:60PPy exhibits a smaller crystallite size (Table 4.6) due to the significant influence of the higher concentration of polypyrrole (PPy) in the composite. PPy is an amorphous, conducting polymer that tends to inhibit the crystal growth of SnO_2 nanoparticles during synthesis. As the PPy content increases, it acts as a physical barrier around growing SnO_2 crystals, restricting their coalescence and agglomeration. This capping effect disrupts the regular crystal lattice formation, leading to smaller and more dispersed SnO_2 crystallites. Furthermore, the interaction between PPy chains and SnO_2 particles introduces structural disorder, increasing strain and defects, which also contributes to peak broadening in the XRD pattern and hence a reduction in apparent crystallite size as calculated by Scherrer's formula. Therefore, in the 40SnO_2:60PPy composition, the dominant PPy matrix effectively limits SnO_2 crystal growth, resulting in the observed smaller crystallite size [13-14].

B. SEM Analysis:

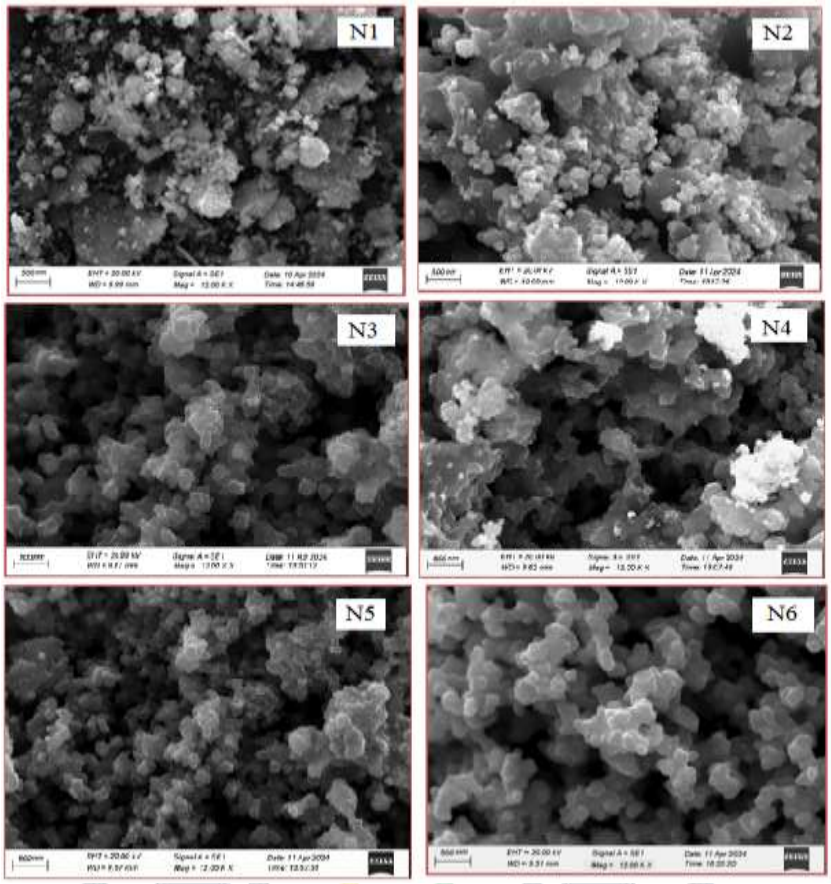

Fig. 3 : SEM Pictures of N1 to N6 sensors

Thus, it is observed that the 40SnO_2:60PPy composite achieves an optimal balance between the inorganic SnO_2 nanoparticles and the conductive polymer matrix. At this composition, PPy prevents excessive agglomeration of SnO_2, promoting fine dispersion, while also forming an interconnected network that introduces ample voids and open channels. Unlike the 80% or 20% PPy samples, where the structure is either too dense or overly polymer-dominant, the 60% PPy provides enough matrix flexibility to allow expansion, creating maximum porosity and surface area, ideal for ammonia gas sensor applications [15-16]. The porosity, particle size and morphology are listed in table 3.

Table 3: Particle size and morphology of Second (N) series.

Sample Code	Composition (SnO_2:PPy)	Porosity	Particle Size (nm)	Morphology
N1	100:00	Very low	60–100	Low dense
N2	80:20	Low	50–80	Dense
N3	60:40	Moderate	40–60	Loosely
N4	40:60	Very High	20–40	Open, sponge-like porous network
N5	20:80	High (slightly reduced)	30–50	Polymer-dominant, smoother with embedded particles
N6	00:100	Comparatively low	70–110	Slightly low dense

C. Sensitivity measurement:

Sensitivity [17-18] or response of the sensors is measured in terms of change in resistance in the environment of ammonia gas with respect to the resistance of the sensor in air surrounding.
Mathematically, sensitivity is expressed as:

$$S = \left(\frac{R_g - R_a}{R_a}\right) = \left(\frac{\Delta R}{R_a}\right)$$

Where, R_g = sensor resistance in presence of gas
R_a = sensor resistance in the environment of air.

The fabricated sensors showed maximum variations in the resistance [19-20] at room temperature i.e. 300 K, therefore, the sensivityvity was determined at room temperature.

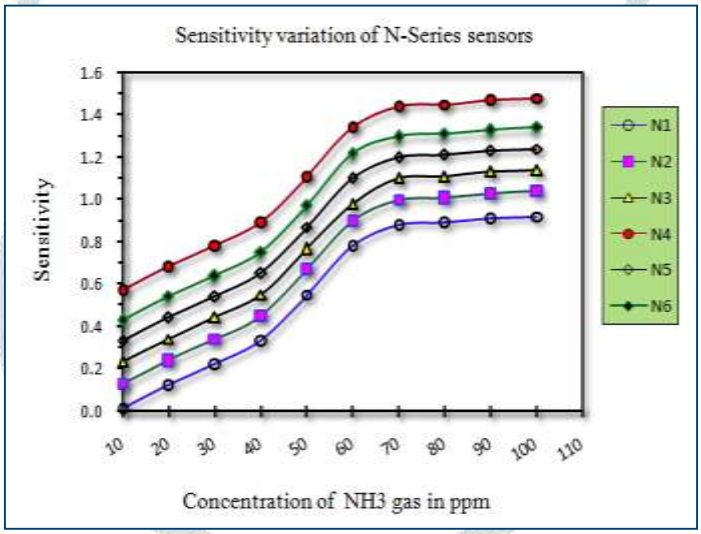

Fig. 4 : Variation of sensitivity of N1 to N6 sensors at Room Temperature

Fig. 4 depicts the sensitivity variation of N1 to N6 sensors with increasing concentrations of NH_3 gas (from 10 to 100 ppm) at room temperature. All sensors show a consistent increase in sensitivity with higher NH_3 concentration, indicating enhanced gas interaction. Among the series, N4 exhibits the highest sensitivity, reaching approximately 1.45 at 70 ppm, demonstrating superior gas detection capability, likely due to optimal material composition, enhanced surface reactivity. N6 and N5 follow closely behind, with good sensitivity performance, suggesting efficient sensing layers or heterojunction effects. N3 shows moderate sensitivity, while N1 and N2 exhibit the lowest sensitivity across all concentrations, indicating relatively weaker response to ammonia exposure. The difference in sensitivity across sensors likely arises from variations in material ratios, microstructure, and porosity, influencing gas adsorption and electron transfer efficiency [21-22].

IV. Conclusion:

XRD patterns of composites of SnO_2 and PPy depicted the tetragonal structure and crystalline size was found to be least, 38.2 nm for $40SnO_2$:60ZnO composition i.e. N4 sensor. Also N4 sensor exhibited very high porosity with particle size 20 to 40 nm due to Open, sponge-like porous network morphology. Among the N-series, N4 manifested the highest sensitivity, reaching approximately 1.45 at 70 ppm at room temperature, demonstrating superior gas detection capability, likely due to enhanced surface reactivity. Thus N4 sesnor is best to detect ammonia gas at room temperature.

V. Acknowledgment:

The authors sincerely acknowledge Vidya Bharati Mahavidyalaya, Amravati and Vidya Bharati Madhyamik Vidyalaya, Amravati for providing the necessary facilities, resources, and a supportive environment to carry out this research work. The constant encouragement, infrastructure support, and access to institutional resources were invaluable in the successful completion of this study.

References:

1. Sayali Atkare, Som Datta Kaushik, Shweta Jagtap, Chandra Sekhar, Room‐temperature chemiresistive Ammonia sensors based on 2D MXenes and hybrids. Dalton Trans., **2023**, 52, 13831–13851.

2. Jose Carlos Santos-Ceballos, Foad Salehni, Frank Guell Alfonso Romero, Xavier Vilanov, Eduard Llobet, Room-Temperature Ammonia Sensing Using Polyaniline-Coated Laser-Induced Graphene, Sensors, 24, **2024**, 1-16.

3. Y Xiao, Y X Pang, Y Yan, P Qian, H Zhao, S Manickam, Wu T, C H Pang, Synthesis and Functionalization of Graphene Materials for Biomedical Applications: Recent Advances, Challenges, and Perspectives. Adv. Sci., **2023**, 10, 2205292

4. V B Mbayachi, E Ndayiragije, T Sammani, S Taj, E R Mbuta, A U Khan, Graphene Synthesis, Characterization and Its Applications: A Review. Results Chem., **2021**, 3, 100163.

5. Pan, J.; Ganesan, R.; Shen, H.; Mathur, S. Plasma-modified SnO2 nanowires for enhanced gas sensing. J. Phys. Chem. C, **2010**, 114, 8245-8250.

6. Wang, Z.X.; Liu, L. Synthesis and ethanol sensing properties of Fe-doped SnO2 nanofibers. Mater. Lett., **2009**, 63, 917-919.

7. Van Hieu, N.; Kim, H.R.; Ju, B.K.; Lee, J.H. Enhanced performance of SnO_2 nanowires ethanol sensor by functionalizing with La_2O_3. Sens. Actuators B, **2008**, 133, 228-234.

8. Peng Wu, Yi Li, Song Xiao, Junyi Chen, Ju Tang, Dachang Chen, Xiaoxing Zhang, "Interaction Mechanisms of Ammonia and Tin Oxide: A Combined Analysis Using Single Nanowire Devices and DFT Calculations", The Journal of Physical Chemistry 2023, 117, 7, 3520–3526.

9. M. Hjiri, S. Algessair, R. Dhahri, H. B. Albargi, N. Ben Mansour, A. A. Assadi & G. Neri, Ammonia gas sensors based on undoped and Ca-doped ZnO nanoparticles", RSC Advances, **2024**, 14, 5001–5011.

10. Anju Thomas and Kalainathan Sivaperuman, Carbon and cobalt co-doped ZnO thin films for highly sensitive and selective ammonia detection at room temperature, Mater. Adv., **2025**, 6, 629-640

11. Khong Van Nguyen , Bui Ha Trung , Chu Van Tuan , Cong Doanh Sai , Tung Duy Vu , Tran Trung , Giang Hong Thai , Ho Truong Giang and Hoang Thi Hien, Ammonia gas-sensing behavior of uniform nanostructured PPy film prepared by simple-straightforward in situ chemical vapor oxidation, Open Physics **2023**; 21, 1-13.

12. Yawale S. P, Yawale S. S, Lamdhade G. T., Hybrid Composites of Poly (diphenylamine sulfonic acid) and nano-Alumina for Impedimetric Humidity Sensors, Sensors and Actuators A, **2007,** 135, 388–393.

13. Petrov V. V.; Sysoev V. V.; Starnikova A. P.; Volkova M. G.; Kalazhokov Z. K.; Storozhenko V. Y.; Khubezhov S. A.; Bayan E. M. "Synthesis, Characterization and Gas Sensing Study of ZnO–SnO_2 Nanocomposite Thin Films." *Chemosensors*, **2021**, *9* (6): Article 124.

14. Aasim Hussain, Shumaila Akram, Anju Dhillon: Comparative Study of Polypyrrole/Zinc Oxide Nanocomposites Synthesized by Different Methods, Research Gate Publication, **2023**, 601-607.

15. Baruah, S.; Nayak, B.; Puzari, A. "Physicochemical Characterization of SnO_2 Grafted Poly p-Phenylenediamine Hybrid Nanocomposites and Their Enhanced Antibacterial Properties." Journal of Polymer Research, **2021**, 28:120 (page 120).

16. Yang, Y.; Kim, D.-H.; Kim, W.-S.; Kang, T.J.; Lee, B.Y.; Hong, S.; Kim, Y.H.; Hong, S.-H. H_2 sensing characteristics of SnO_2 coated single wall carbon nanotube network sensors. Nanotechnology, **2010**, 21, 215501.

17. Gao, T.; Wang, T.H. Sonochemical synthesis of SnO_2 nanobelt/CdS nanoparticle core/shell heterostructures. Chem. Commun., **2004**, 22, 2558-2559.

18. Han, X.M.; Zhang, B.; Guan, S.K.; Liu, J.D.; Zhang, X.; Chen, R.F. Gassensing properties of SnO_2 nanobelts synthesized by thermal evaporation of Sn foil. J. Alloys Comp., **2008**, 461, L26-L28.

19. Kumar, S.; Peng, Z.C.; Shin, H.; wang, Z.L.; Hesketh, P.J. AC dielectrophoresis of tin oxide nanobelts suspended in ethanol: manipulation and visualization. Anal. Chem., **2010**, 82, 2204-2212.

20. Huang, H.; Lee, Y.C.; Tan, O.K.; Zhou, W.; Peng, N.; Zhang, Q. High sensitivity SnO_2 single-nanorod sensors for the detection of H_2 gas at low temperature. Nanotechnology, **2009**, 20, 115501.

21. Huang, J.; Matsunaga, N.; Shimanoe, K.; Yamazoe, N.; Kunitake, T. Nanotubular SnO_2 templated by cellulose fibers: Synthesis and gas sensing. Chem. Mater., **2005**, 17, 3513-3518.

22. Prabakaran, K.; Sufiyan, K. T. M.; Kumar, S.; et al. "Synthesis of Zinc Oxide and Tin Oxide (ZnO/SnO_2) Nanocomposite for Photoanode Applications in Dye Sensitized Solar Cell." *Journal of Materials Science: Materials in Electronics*, **2024**, vol. 35, p. 1993.